Supporting Information

Miura et al. 10.1073/pnas.1303111110

SI Materials and Methods

Introduction of Point Mutations into the *RAD52* Locus. The mutant lacking the entire *RAD52*-coding region with the *URA3* selective marker, *rad52Δw::URA3*, was generated by PCR on pYES2 (Invitrogen) plasmid DNA (with *URA3*) with the primers PRI1043/PRI1044 (Table S2), and transformation of the resultant *rad52Δw::URA3* DNA fragment into the wild-type strain KTYY90 (for SDSA/NHEJ assay), with selection for Ura$^+$. To enhance the replacement reaction between the introduced *rad52* mutant DNA and the *rad52Δw::URA3* allele, the pGADT7AD-*RAD52* (with *LEU2*) plasmid, containing the region from the 67th codon to the 504th (last sense) codon, was constructed by PCR on genomic DNA from W303α with PRI890/PRI891 (Table S2), and the fragment was inserted into the pGADT7AD (Clontech) plasmid vector, using an In-Fusion HD Cloning Kit (Clontech). The plasmid was then transformed into the strain with the *rad52Δw::URA3* allele. The replacement DNA with the *rad52-K117D, R148D* allele was generated by PCR on the pNS188 plasmid DNA bearing this allele [a gift from N. Arai (1)] with the PRI1045/PRI1046 primers (Table S2) and replaced with *rad52Δw::URA3* in the presence of the *RAD52* plasmid, followed by selection for 5FOA resistance. The replacement of the *rad52* mutant DNA with the whole deletion allele was confirmed by PCR with the outside primers of PRI1045/PRI1046. The *RAD52* plasmid DNA was cured (loss of Leu$^+$ phenotype). The sequences of the introduced base substitutions and the other regions were confirmed by sequencing the amplified *rad52* mutant DNA with the outside primers of PRI1045/PRI1046 from the genomic DNA.

Introduction of Point Mutations and In-Frame Deletions into the *SRS2* Locus. The mutant lacking the entire *SRS2*-coding region with the *URA3* selective marker, *srs2Δw::URA3*, was generated by PCR on pYES2 plasmid DNA (with *URA3*) with the PRI809/PRI810 primers (Table S2), and the resultant *srs2Δw::URA3* DNA fragment was transformed into the wild-type strains W303α (for the targeted integration assay) and KTYY90 (for SDSA/NHEJ assay), with Ura$^+$ selection. The inverse PCR-based mutagenesis method (KOD-Plus-Mutagenesis Kit; TOYOBO) was performed on pCRBluntIITOPO-*SRS2* plasmid DNA, which was constructed by PCR on genomic DNA from W303α with the PRI742/PRI743 primers (Table S2) and inserting into pCRBluntIITOPO (Invitrogen), with the forward and reverse primers situated just outside a designed deletion, or with the forward primer and its adjacent reverse primer, with either including the designed base substitution. The primer sequences for the designed mutants are described in Tables S1 and S2. For the K41M amino acid change in the Srs2 protein, the base substitution (underlined) from AAG to ATG was designed. For the K41A amino acid change in the Srs2 protein, the base substitutions (underlined) from AAG to GCT were designed. The mutant *srs2* plasmid obtained was used as the PCR-template DNA to create the replacement DNA by PCR with the primers PRI742/PRI743, and the replacement DNA was transformed into strains with *srs2Δw::URA3*, followed by selection for 5FOA resistance. The replacement of the *srs2* mutant DNA with the whole deletion allele was confirmed by PCR with the outside primers of PRI742/PRI743. The sequences of the introduced deletions, the base substitutions, and the other regions were confirmed by sequencing the *srs2* mutant DNA, amplified with the outside primers of PRI742/PRI743 from the genomic DNA.

Introduction of Point Mutations into the *POL30 (PCNA)* Locus. First, the pYES2.1TOPOTA-*GAL1pro-POL30-TT* plasmid was constructed by PCR on genomic DNA from W303α with the PRI972/PRI973 primers, and insertion of the resultant *POL30* DNA fragment into the pYES2.1TOPOTA (Invitrogen) plasmid vector. Subsequently, the pYES3/CT-*GAL1pro-POL30-TT* (Trp$^+$) plasmid DNA was constructed by PCR on the pYES2.1TOPOTA-*GAL1pro-POL30-TT* plasmid DNA with the PRI1017/PRI1018 primers (Table S2), and insertion of the resultant *POL30* fragment into the pYES3/CT (Invitrogen) plasmid vector, using an In-Fusion HD Cloning Kit (Clontech). The resultant plasmid was transformed into the wild-type strain KTYY90 (for SDSA/NHEJ assay) by selection for Trp$^+$. The mutant lacking the entire *POL30*-coding region with the *URA3* selective marker, *pol30Δw::URA3*, was generated by PCR on pYES2 plasmid DNA (with *URA3*), with the PRI1008/PRI1009 primers (Table S2), and transformation of the resultant *pol30Δw::URA3* DNA fragment into the pYES3/CT-*GAL1pro-POL30-TT* (Trp$^+$)-bearing KTYY90 strain, with selection for Ura$^+$. The inverse PCR-based mutagenesis method was performed on the pYES2.1TOPOTA-*GAL1pro-POL30-TT* plasmid DNA, with the forward primer including the base substitution (underlined) from AAA to AGA and its adjacent reverse primer for the K164R amino acid change in the PCNA protein, to create the pYES2.1TOPOTA-*GAL1-pro-pol30-K164R-TT* plasmid. The same method was also performed on pYES2.1TOPOTA-*GAL1pro-pol30-K164R-TT* plasmid DNA, with the forward primer including the base substitutions (underlined) from AAG to AGA and the adjacent reverse primer for the K127R amino acid change in PCNA protein, to create the pYES2.1TOPOTA-*GAL1pro-pol30-K127R, K164R-TT* plasmid. The obtained *pol30* (*pcna*) mutant plasmid was used as the PCR-template DNA to generate the replacement DNA by PCR with the primers PRI1010/PRI1011 (Table S2), and the replacement DNA was transformed into the strain with *pol30Δw::URA3*, followed by selection for 5FOA resistance. The resultant replacement of the *pol30* mutant DNA with the whole deletion allele was confirmed by PCR, with the outside primers of PRI1010/PRI1011. The *POL30* plasmid DNA was cured (loss of Trp$^+$ phenotype). The sequences of the base substitutions and the other regions were confirmed by sequencing the amplified *pol30* mutant DNA, with the outside primers of PRI1010/PRI1011, from the genomic DNA.

1. Arai N, et al. (2011) Vital roles of the second DNA-binding site of Rad52 protein in yeast homologous recombination. *J Biol Chem* 286(20):17607–17617.

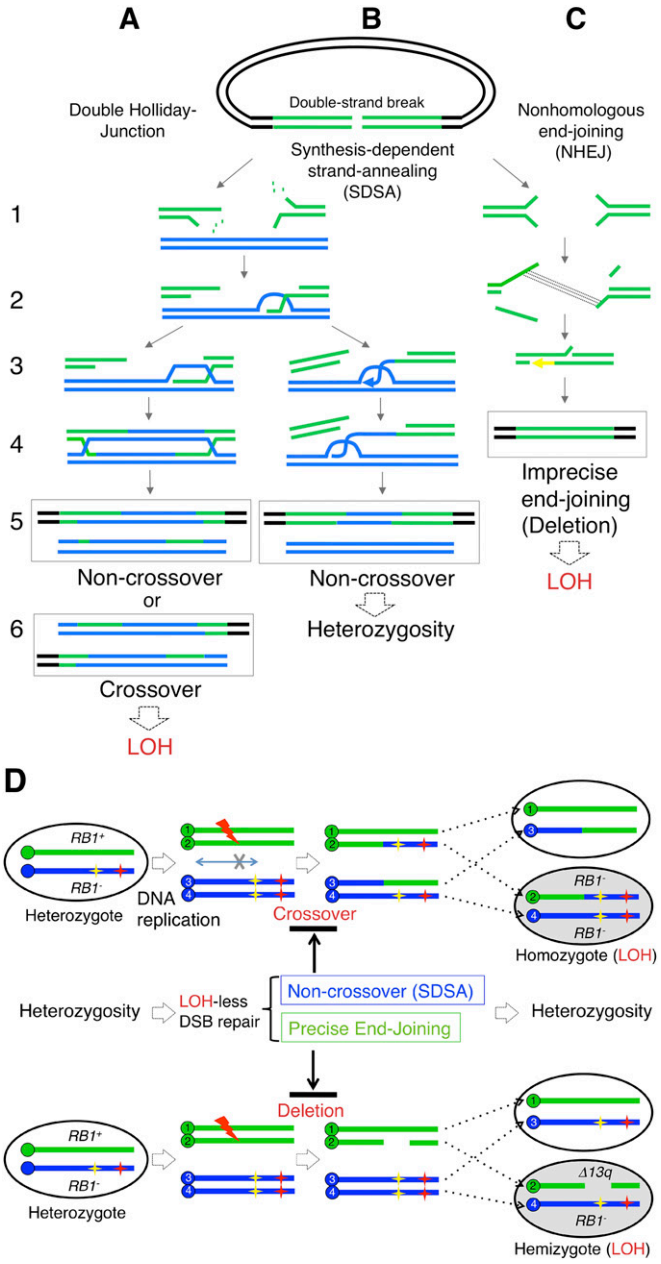

Fig. S1. DNA double-strand break repair pathways and loss of heterozygosity. (*A*) Double Holliday junction-mediated homologous recombination, involving the resolution of double Holliday-junction intermediates (*A, 4*), generates noncrossovers (*A, 5*), or crossovers (*A, 6*), causing loss of heterozygosity (1). (*B*) SDSA-mediated homologous recombination, involving bubble migration (*B, 2–4*), generates only noncrossovers (*B, 5*), maintaining heterozygosity (1). (*C*) NHEJ generates either precise end-joining or imprecise end-joining (*C, 4*), causing loss of heterozygosity, based on a microhomology-mediated end-joining mechanism (2). (*D*) Suppression of crossovers and deletions by promoting loss-of-heterozygosity–less DSB repair, SDSA, and precise end-joining. When a double-strand break is induced anywhere between a centromere and specific loci of a chromosome in 4*n*-stage somatic cells heterozygous for the loci, such as a recessive mutation of the tumor suppressor gene, *retinoblastoma 1*, *RB1*$^{-}$ (yellow cross) and a recessive mutation of another locus (red cross) in the distal end of the human 13th chromosome, double Holliday junction-mediated homologous recombination and imprecise end-joining often produce a crossover between homologous chromosomes (*Top*) and a deletion (*Bottom*), respectively. Upon cell division, these reactions cause homozygous status including *RB1*$^{-}$/*RB1*$^{-}$ in the distal loci (*Top*) and hemizygous status including *RB1*$^{-}$/*Δ13q* in the in-deletion locus (*Bottom*), respectively, and both cause loss of heterozygosity. The SDSA pathway producing only the noncrossover type and the precise end-joining pathway are not associated with flanking exchange and deletion around the double-strand break, respectively. Thus, these pathways avoid the double-strand break-induced loss of heterozygosity in somatic cells (*Middle*). LOH, loss of heterozygosity.

1. Miura T, et al. (2012) Homologous recombination via synthesis-dependent strand annealing in yeast requires the Irc20 and Srs2 DNA helicases. *Genetics* 191(1):65–78.
2. Hicks WM, Kim M, Haber JE (2010) Increased mutagenesis and unique mutation signature associated with mitotic gene conversion. *Science* 329(5987):82–85.

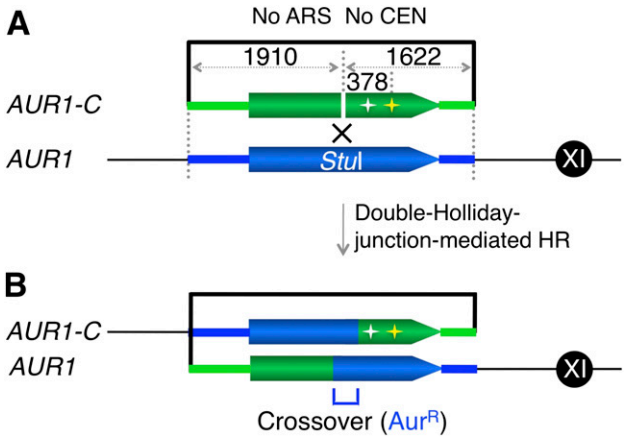

Fig. S2. Targeted integration of *AUR1-C* DNA into the *AUR1* locus via double Holliday junction-mediated homologous recombination. (*A*) pAUR101, which bears the dominant *AUR1-C* allele conferring resistance to Aureobasidin A (Aur^R), lacks a centromere (CEN) and an autonomous replication site (ARS) (1). When the *AUR1-C* plasmid DNA is cleaved by the StuI enzyme, one end of the double-strand break is 133 bp away from the 1-base substitution (underlined) in the 158th codon [white cross; TTT (F) to TAT (Y)] and 378 bp away from the 2-base substitution (underlined) in the 240th codon [yellow cross; GCT (A) to TGT (C)], of *AUR1-C*. The StuI-cleaved 5′ end and 3′ end share 1,910-bp homology and 1,622-bp homology with the *AUR1* locus (chromosome XI), respectively. (*B*) Targeted-integration products via double Holliday junction-mediated homologous recombination, conferring Aur^R (1). In this assay, the majority of the targeted integration products are the crossover type, with a minority of the noncrossover type with conversions across the *AUR1-C* mutations. The targeted integration of the StuI-cut pAUR101 DNA is completed only via double Holliday junction-mediated homologous recombination to give rise to the targeted integrants conferring Aur^R because the DNA recircularized via SDSA or NHEJ lacks CEN and ARS and thus can never confer Aur^R. If a crossover occurs between the double-strand break and the 1-base substitution in the 158th codon of *AUR-1C*, then the resultant targeted integrants confer Aur^R. In a targeted integration assay with the wild-type strain, 45 out of 48 Aur^R progeny had the tandem-duplication (or multiplication) configuration, which were the crossover type. Three had the singlet configuration, of which 2 were the noncrossover type with a conversion across the 2-base substitution in the 240th codon of *AUR1-C*; and 1 was the noncrossover type with a shorter conversion across the 1-base substitution in the 158th codon of *AUR1-C*. This assay enables the quantification of the targeted integration products, including crossover and noncrossover types, which are completed via the double Holliday junction-mediated homologous recombination.

1. Miura T, et al. (2012) Homologous recombination via synthesis-dependent strand annealing in yeast requires the Irc20 and Srs2 DNA helicases. *Genetics* 191(1):65–78.

Table S1. Description of *Saccharomyces cerevisiae* strains used

Strain	Genotype	Source or PCR primers* used for strain constructions
W303α	MATα *leu2-3, 112 trp1-1 ura3-1 his3-11, 15 ade2-1 can1-100 RAD5*	WT strain in the targeted integration assay (1)
KITTM415	W303α, *srs2Δw::TRP1*	PRI1092/PRI868 for *srs2Δw::TRP1*
KITTM244	W303α, *srs2Δw::URA3*	PRI809/PRI810 for *srs2Δw::URA3*
KITTM441	W303α, *srs2Δ783–998* (5FOA^R from KITTM244)	PRI977/PRI1093 for *srs2Δ783–998*
KITTM577	W303α, *srs2Δ783–859* (5FOA^R from KITTM244)	PRI1138/PRI1093 for *srs2Δ783–859*
KITTM581	W303α, *srs2Δ860–998* (5FOA^R from KITTM244)	PRI977/PRI1139 for *srs2Δ860–998*
KITTM447	W303α, *srs2ΔPIP (Δ1149–1156)* (5FOA^R from KITTM244)	PRI1075/PRI1074 for *srs2ΔPIP*
KITTM451	W303α, *srs2ΔSIM (Δ1169–1174)* (5FOA^R from KITTM244)	PRI1073/PRI1072 for *srs2ΔSIM*
KITTM507	W303α, *srs2ΔPIP, ΔSIM (Δ1149–1156, Δ1169–1174)* (5FOA^R from KITTM244)	PRI1073/PRI1072 for *srs2ΔPIP, ΔSIM*
KITTM401	W303α, *srs2-K41M* (5FOA^R from KITTM244)	PRI1012/PRI1013 for *srs2-K41M*
KITTM781	W303α, *srs2-K41A* (5FOA^R from KITTM244)	PRI1012/PRI1287 for *srs2-K41A*
KTYY90	*MATα leu2-3, 112 trp1-1 5′Δ(::HIS3)-ura3 his3-11,15 ade2-1 can1-100 RAD5 AUR1-C-(pUCOri-Amp^R-ura3-3′Δ)-AUR1*	WT strain in the SDSA or NHEJ assay (2)
KITTM377	KTYY90, rad52Δw::URA3	PRI1043/PRI1044 for *rad52Δw::URA3*
KITTM419	KTYY90, *rad52-K117D, R148D* (5FOA^R from KITTM377 with pGADT7AD::*RAD52* (Leu$^+$) and plasmid-cured)	PRI1045/PRI1046 for *rad52-K117D, R148D* (3)
KTYY142	KTYY90, *rad52ΔKO::KAN*	(2)
KITTM15	KTYY90, *rad54ΔKO::KAN*	PRI704/PRI705 for *rad54ΔKO::KAN*
KTYY137	KTYY90, *rad51ΔKO::KAN*	PRI161/PRI162 for *rad51ΔKO::KAN*
KITTM587	KTYY90, *rad51Δw::HYG*	PRI1134/PRI1135 for *rad51Δw::HYG*
KTYY120	KTYY90, *lig4ΔKO::KAN*	(2)
KITTM331	KTYY90, *lig4ΔKO::KAN rad51ΔKO::HYG*	PRI161/PRI162 for *rad51ΔKO::HYG*
KITTM445	KTYY90, *rad52-K117D, R148D rad51ΔKO::HYG* (Hyg^R from KITTM419 with pGADT7AD::*RAD52* (Leu$^+$) and plasmid-cured)	PRI161/PRI162 for *rad51ΔKO::HYG*
KITTM417	KTYY90, *srs2Δw::TRP1*	PRI1092/PRI868 for *srs2Δw::TRP1*
KITTM493	KTYY90, *srs2Δw::TRP1 rad51ΔKO::HYG*	PRI161/PRI162 for *rad51ΔKO::HYG*
KITTM171	KTYY90, *srs2Δw::URA3*	PRI809/PRI810 for *srs2Δw::URA3*
KITTM443	KTYY90, *srs2Δ783–998* (5FOA^R from KITTM171)	PRI977/PRI1093 for *srs2Δ783–998*
KITTM579	KTYY90, *srs2Δ783–859* (5FOA^R from KITTM171)	PRI1138/PRI1093 for *srs2Δ783–859*
KITTM583	KTYY90, *srs2Δ860–998* (5FOA^R from KITTM171)	PRI977/PRI1139 for *srs2Δ860–998*
KITTM449	KTYY90, *srs2ΔPIP (Δ1149–1156)* (5FOA^R from KITTM171)	PRI1075/PRI1074 for *srs2ΔPIP*
KITTM453	KTYY90, *srs2ΔSIM (Δ1169–1174)* (5FOA^R from KITTM171)	PRI1073/PRI1072 for *srs2ΔSIM*
KITTM509	KTYY90, *srs2ΔPIP, ΔSIM (Δ1149–1156, Δ1169–1174)* (5FOA^R from KITTM244)	PRI1073/PRI1072 for *srs2ΔPIP, ΔSIM*
KITTM403	KTYY90, *srs2-K41M* (5FOA^R from KITTM171)	PRI1012/PRI1013 for *srs2-K41M*
KITTM783	KTYY90, *srs2-K41A* (5FOA^R from KITTM171)	PRI1012/PRI1287 for *srs2-K41A*
KITTM375	KTYY90, *siz1Δw::HYG*	PRI1039/PRI1040 for *siz1Δw::HYG*
KITTM353	KTYY90, *pol30* (*pcna*)*Δw::URA3* [pYES3-*GAL1pro-POL30-TT* (Trp$^+$)]	PRI1008/PRI1009 for *pol30Δw::URA3*
KITTM745	KTYY90, *pol30* (*pcna*)*-K164R* (5FOA^R from KITTM353 and plasmid-cured)	PRI1006/PRI1007 for *pol30-K164R*
KITTM747	KTYY90, *pol30* (*pcna*)*-K127R, K164R* (5FOA^R from KITTM353 and plasmid-cured)	PRI1130/PRI1131 for *pol30-K127R, K164R*
KITTM381	KTYY90, *rad6Δw::HYG*	PRI1047/PRI1048 for *rad6Δw::HYG*
KITTM759	KTYY90, *pol30* (*pcna*)*-K164R rad6Δw::HYG*	PRI1047/PRI1048 for *rad6Δw::HYG*
KITTM573	KTYY90, *siz1Δw::HYG rad6Δw::KAN*	PRI1047/PRI1048 for *rad6Δw::KAN*
KITTM427	KTYY90, *siz1Δw::HYG srs2Δw::TRP1*	PRI1092/PRI868 for *srs2Δw::TRP1*
KITTM761	KTYY90, *pol30* (*pcna*)*-K164R srs2Δw::TRP1*	PRI1092/PRI868 for *srs2Δw::TRP1*
KITTM435	KTYY90, *rad6Δw::HYG srs2Δw::TRP1*	PRI1092/PRI868 for *srs2Δw::TRP1*

ΔKO shows the absence of most of the coding region, and *Δw* shows the absence of the entire coding region from the initiation codon to the last sense codon. *pol30* mutants are indicated as *pol30* (*pcna*) to show that *pol30*s are the mutants in the PCNA-encoding gene in the text and this table.
*The sequences of the PCR primers used to construct each mutant gene are shown in Table S2.

1. Thomas BJ, Rothstein R (1989) Elevated recombination rates in transcriptionally active DNA. *Cell* 56(4):619–630.
2. Miura T, et al. (2012) Homologous recombination via synthesis-dependent strand annealing in yeast requires the Irc20 and Srs2 DNA helicases. *Genetics* 191(1):65–78.
3. Arai N, et al. (2011) Vital roles of the second DNA-binding site of Rad52 protein in yeast homologous recombination. *J Biol Chem* 286(20):17607–17617.

Table S2. The list of primers used for strain construction and plasmid construction

Primer no.	Sequences of forward (F) and reverse (R) primers
One-step gene disruption and gene replacement	
PRI161	F: AACGGTTCGTTGATGTCCACTGTACCAGCAGACCTTTCACAG-5′HYG or 5′KAN
PRI162	R: TCACCAACACCATCTTCATAGATCGCGAACACACATTCAGC-3′HYG or 3′KAN
PRI704	F: TTAGCTCTATTTCAAGGTACCATATATATTTCCTTATAACTG-5′*loxP*-KAN
PRI705	R: TATAAGTACATGTATGTAAGAGATCAATGTGAAATATATTGA-3′*loxP*-KAN
PRI742	F: AAGATACATAGGGTCAGGC
PRI743	R: TTCTTGTTATCAGCCAGTTGG
PRI809	F: TCATTCCAATTTGATCTTTCTTCTACCGGTACTTAGGGATAGCA-5′URA3
PRI810	R: ACCGCCTCCAATAGTTGACGTAGTCAGGCATGAAAGTGCTACTA-3′URA3
PRI1008	F: CAACAAGCAGCAAGCACTAAGTACGCAGTCAAAAGAGAGAAAAA-5′URA3
PRI1009	R: GTTTATTATTTTTAGTATACAACTATATAGATAATTTACATTTA-3′URA3
PRI1010	F: CAACAAGCAGCAAGCACTAAGTACGCAGTCAAAAGAGAGAAAAAATGTTAGAAGCAAAATTTGAAGAAGCATCCC
PRI1011	R: GTTTATTATTTTTAGTATACAACTATATAGATAATTTACATTTATTCTTCGTCATTAAATTTAGGAGCC
PRI1039	F: ACTCCAACTCAAACAGTTGAGTGTTCCATATACATTCTGTTTCA-5′HYG
PRI1040	R: ATGAAAGAGCTGGACGGAACCGTCCAATTTTAGCCTCGTTTTTA-3′HYG
PRI1043	F: TGCCAAGAACTGCTGAAGGTTCTGGTGGCTTTGGTGTGTTGTTG-5′URA3
PRI1044	R: TAATGATGCAAATTTTTTATTTGTTTCGGCCAGGAAGCGTTTCA-3′URA3
PRI1045	F: TGCCAAGAACTGCTGAAGGTTCTGGTGGCTTTGGTGTGTTGTTGATGAATGAAATTATGGATATGG
PRI1046	R: TAATGATGCAAATTTTTTATTTGTTTCGGCCAGGAAGCGTTTCAAGTAGGCTTGCGTGCATGCAGG
PRI1047	F: CAAAGATTATTTTTAGGCAGACAGAGACTAAAAGATAAAGCGTC-5′HYG
PRI1048	R: TATCGGCTCGGCATTCATCATTAAGATTCTTTTGATTTTTCTCA-3′HYG
PRI1092	F: CATTCCAATTTGATCTTTCTTCTACCGGTACTTAGGGATAGCAA-5′TRP1
PRI868	R: TAAACCGCCTCCAATAGTTGACGTAGTCAGGCATGAAAGTGCTA-3′TRP1
PRI1134	F: AGACGTAGTTATTTGTTAAAGGCCTACTAATTTGTTATCGTCAT-5′HYG
PRI1135	R: AGTAAACCTGTGTAAATAAATAGAGACAAGAGACCAAATACCTA-3′HYG
Inverse PCR for in-frame deletion and base substitution	
PRI977	F: GAATACTCCAATAAATCAGGGC
PRI1138	F: GAAAAATCACGCCCATCC
PRI1093	R: CGGCTTTTTGTTCAAAATTCGG
PRI1139	R: AATAAGTTTCTTCTGTGGG
PRI1006	F: **AGA**GAAACAATAAAGTTTGTAGCTGACGG
PRI1007	R: GGTGATCATGATATTAATAGAATCACTCAATTGGG
PRI1012	F: ACTAAGGTTTTAACTTCAAGAGTAGCG
PRI1013	R: **CAT**CCCTGTGCCGGGACCGGC
PRI1287	R: **AGC**CCCTGTGCCGGGACCGGC
PRI1073	F: TAGTAGCACTTTCATGCCTG
PRI1072	R: ACCGTTGTTTAATTTTGACTTTTTTTTCGCACG
PRI1075	F: TCACGTGCGAAAAAAAAGTCAAAATTAAACAACGG
PRI1074	R: ACTTGATGCAGGTTCATTCTTCACC
PRI1130	F: **AGA**ATTGAAGAATTACAGTACGACTCC
PRI1131	R: TAAGAAATCAGCATCGATATCC
Plasmid construction	
PRI890	F: gtaccagattacgctcatatgATCTCCAAGAGAGTTGGGTTTGG
PRI891	R: atgcccacccgggtggaattcTCAAGTAGGCTTGCGTGCATGC
PRI972	F: CAAGCACTAAGTACGCAGTC
PRI973	R: TTCTTCGTCATTAAATTTAGGAGCC
PRI1017	F: actatagggaatattaagcttCAAGCACTAAGTACGCAGTC
PRI1018	R: gaagggccctctagactcgagTTCTTCGTCATTAAATTTAGGAGCC

Bold letters in sequences indicate designed base substitutions to generate amino acid changes. Lowercase letters indicate sequences overlapping with the cloning sites of plasmid vectors, which are necessary for the in-fusion cloning method. The sequences located on the 5′ ends and the 3′ ends of the selective marker genes in the homology arm-trailed primers for the PCR-based one-step gene disruption method are shown below:

5′URA3 of pYES2: AGCTTTTCAATTCAATTCATC

3′URA3 of pYES2: TACTCTTCCTTTTTCAATGGG

5′HYG of pAG34-HYG or 5′KAN of pFA6a-KanMX4: GGTTAATTAAGGCGCGCC

5′HYG of pAG34-HYG or 5′KAN of pFA6a-KanMX4: ATCGATGAATTCGAGCTCG

5′TRP1 of pAS2-1: CGGCATCAGAGCAGATTG

3′TRP1 of pAS2-1: CGCATAGATCGGCAAGTGCAC

5′*loxP*-KAN: ATAACTTCGTATAATGTATGCTATACGAAGTTATGGTTAATTAAGGCGCGCC

3′*loxP*-KAN: ATAACTTCGTATAGCATACATTATACGAAGTTATATCGATGAATTCGAGCTCG

Table S3. Statistical analysis of SDSA and NHEJ frequencies of the homologous recombination-deficient mutants shown in Fig. 2 *B* and *C*

Relevant genotype (strain)	Transformation, *n*	Mean ± SD of SDSA frequency, % (*P* value from two-tailed Student's *t* test)	Mean ± SD of NHEJ frequency, % (*P* value from two-tailed Student's *t* test)
WT (KTYY90)	7	4.2 ± 0.44	1.0 ± 0.13
rad52-K117D, R148D (KITTM419)	5	1.3 ± 0.064 (4.5E−8)	1.4 ± 0.12 (2.7E-4)
rad52ΔKO (KTYY142)	3	ND (NT)	0.99 ± 0.27 (0.92)
rad54ΔKO (KITTM15)	3	0.0016 ± 0.00075 (NT)	0.92 ± 0.21 (0.50)
rad51Δw (KITTM587)	5	ND (NT)	4.3 ± 0.32 (2.1E-10)
rad51ΔKO (KTYY137)	10	0.0010 ± 0.0013 (NT)	4.9 ± 1.0 (3.4E-8)
rad51ΔKO lig4ΔKO (KITTM331)	5	ND (NT)	0.20 ± 0.016 [1.1E-7 (vs. $rad51^{KO}$)]
rad51ΔKO rad52-K117D, R148D (KITTM445)	5	ND (NT)	1.4 ± 0.084 [3.1E-6 (vs. $rad51^{KO}$)]
rad51ΔKO srs2Δw (KITTM493)	5	ND (NT)	1.1 ± 0.035 [1.4E-6 (vs. $rad51^{KO}$)]
WT (*Nru*I) (KTYY90)	5	4.9 ± 0.37	0.99 ± 0.16
rad51ΔKO (*Nru*I) (KTYY137)	4	0.00010 ± 0.00012 (NT)	1.1 ± 0.18 (0.21)
WT (T4 poly) (KTYY90)	4	4.5 ± 0.16	1.3 ± 0.041
rad51ΔKO (T4 poly) (KTYY137)	4	ND (NT)	1.3 ± 0.11 (0.42)

The two-tailed Student's *t* test was performed for the wild-type (WT) strain except where indicated as (vs. genotype). ND, not detected; NT, not statistically tested.

Table S4. Statistical analysis of SDSA frequencies of the various *srs2* mutants shown in Fig. 3*C*

Relevant genotype (strain)	Transformation, *n*	Mean ± SD of SDSA frequency, % (*P* value from two-tailed Student's *t* test)
SRS2 (KTYY90)	6	4.0 ± 0.19
srs2Δw (KITTM417)	6	1.0 ± 0.13 (2.0E-11)
srs2Δ783–998 (KITTM443)	6	0.89 ± 0.088 (4.6E-12)
srs2Δ783–859 (KITTM579)	5	1.5 ± 0.056 (3.0E-10)
srs2Δ860–998 (KITTM583)	5	4.7 ± 0.18 (1.5E-4)
srs2ΔPIP, ΔSIM (KITTM509)	6	1.1 ± 0.085 (8.8E-12)
srs2ΔPIP (KITTM449)	5	1.4 ± 0.14 (7.0E-10)
srs2ΔSIM (KITTM453)	5	1.9 ± 0.12 (4.1E-9)
srs2-K41M (KITTM403)	5	1.2 ± 0.17 (9.6E-10)
srs2-K41A (KITTM783)	5	1.1 ± 0.072 (1.0E-10)

The two-tailed Student's *t* test was performed for the wild-type (*SRS2*) strain.

Table S5. Statistical analysis of the frequencies of double Holliday junction-mediated homologous recombination of the various *srs2* mutants shown in Fig. 3*E*

Relevant genotype (strain)	Transformation, *n*	Mean ± SD of double Holliday junction-mediated homologous recombination frequency, % (*P* value from two-tailed Student's *t* test)
SRS2 (W303α)	7	4.4 ± 0.25
srs2Δw (KITTM415)	5	12 ± 0.72 (1.9E-10)
srs2Δ783–998 (KITTM441)	6	8.7 ± 0.85 (6.8E-8)
srs2Δ783–859 (KITTM577)	5	8.0 ± 0.49 (1.4E-8)
srs2Δ860–998 (KITTM581)	5	3.5 ± 0.23 (3.8E-5)
srs2ΔPIP, ΔSIM (KITTM507)	6	8.1 ± 0.83 (2.7E-7)
srs2ΔPIP (KITTM447)	5	9.3 ± 0.83 (3.5E-8)
srs2ΔSIM (KITTM451)	5	5.1 ± 0.3 (0.0016)
srs2-K41M (KITTM401)	5	5.8 ± 0.32 (1.0E-5)
srs2-K41A (KITTM781)	5	5.9 ± 0.093 (2.7E-7)

The two-tailed Student's *t* test was performed for the wild-type (*SRS2*) strain.

Table S6. Statistical analysis of SDSA frequencies of PCNA modification-related mutants shown in Fig. 4*B*

Relevant genotype (strain)	Transformation, *n*	Mean ± SD of SDSA frequency, % (*P* value from two-tailed Student's *t* test)
WT (KTYY90)	7	4.1 ± 0.23
siz1Δw (KITTM375)	5	1.0 ± 0.064 (5.8E-11)
pol30 (*pcna*)-*K164R* (KITTM745)	5	0.17 ± 0.0048 (3.7E-12) [1.5E-9 (vs. *siz1Δw*)]
pol30 (*pcna*)-*K127R, K164R* (KITTM747)	5	0.17 ± 0.018 (3.8E-12) [2.0E-9 (vs. *siz1Δw*)]
rad6Δw (KITTM381)	5	0.089 ± 0.014 (3.0E-12) [8.6E-10 (vs. *siz1Δw*)]
pol30 (*pcna*)-*K164R rad6Δw* (KITTM759)	5	0.16 ± 0.012 [0.20 (vs. *pol30-K164R*)]
siz1Δw rad6Δw (KITTM573)	5	1.1 ± 0.11 [0.85 (vs. *siz1Δw*)]
siz1Δw srs2Δw (KITTM427)	4	1.0 ± 0.059 [0.65 (vs. *siz1Δw*)]
pol30 (*pcna*)-*K164R srs2Δw* (KITTM761)	5	1.4 ± 0.11 [6.7E-9 (vs. *pol30-K164R*)]
rad6Δw srs2Δw (KITTM435)	4	1.4 ± 0.065 [7.6E-10 (vs. *rad6Δw*)]

The two-tailed Student's *t* test was performed for the wild-type (WT) strain except in cases indicated as (vs. genotype).